Loss of *caspase-2* augments lymphomagenesis and enhances genomic instability in *Atm*-deficient mice

Joseph Puccini[a,b], Sonia Shalini[a], Anne K. Voss[c,d], Magtouf Gatei[e], Claire H. Wilson[a], Devendra K. Hiwase[a], Martin F. Lavin[e,f], Loretta Dorstyn[a,b,g,1], and Sharad Kumar[a,b,g,1,2]

[a]Department of Hematology, Centre for Cancer Biology, SA Pathology, Adelaide, SA 5000, Australia; [b]Department of Medicine, University of Adelaide, Adelaide, SA 5005, Australia; [c]Walter and Eliza Hall Institute of Medical Research, Melbourne, VIC 3052, Australia; [d]Department of Medical Biology, University of Melbourne, VIC 3050, Australia; [e]Queensland Institute of Medical Research, Herston, QLD 4006, Australia; [f]University of Queensland Centre for Clinical Research, Herston, QLD 4006, Australia; and [g]Division of Health Sciences, University of South Australia, Adelaide, SA 5001, Australia

Edited* by Vishva M. Dixit, Genentech, South San Francisco, CA, and approved October 30, 2013 (received for review June 24, 2013)

Caspase-2, the most evolutionarily conserved member of the caspase family, has been shown to be involved in apoptosis induced by various stimuli. Our recent work indicates that caspase-2 has putative functions in tumor suppression and protection against cellular stress. As such, the loss of caspase-2 enhances lymphomagenesis in Eμ-*Myc* transgenic mice, and *caspase-2* KO (*Casp2*$^{-/-}$) mice show characteristics of premature aging. However, the extent and specificity of caspase-2 function in tumor suppression is currently unclear. To further investigate this, ataxia telangiectasia mutated KO (*Atm*$^{-/-}$) mice, which develop spontaneous thymic lymphomas, were used to generate *Atm*$^{-/-}$*Casp2*$^{-/-}$ mice. Initial characterization revealed that *caspase-2* deficiency enhanced growth retardation and caused synthetic perinatal lethality in *Atm*$^{-/-}$ mice. A comparison of tumor susceptibility demonstrated that *Atm*$^{-/-}$*Casp2*$^{-/-}$ mice developed tumors with a dramatically increased incidence compared with *Atm*$^{-/-}$ mice. *Atm*$^{-/-}$*Casp2*$^{-/-}$ tumor cells displayed an increased proliferative capacity and extensive aneuploidy that coincided with elevated oxidative damage. Furthermore, splenic and thymic T cells derived from premalignant *Atm*$^{-/-}$*Casp2*$^{-/-}$ mice also showed increased levels of aneuploidy. These observations suggest that the tumor suppressor activity of caspase-2 is linked to its function in the maintenance of genomic stability and suppression of oxidative damage. Given that ATM and caspase-2 are important components of the DNA damage and antioxidant defense systems, which are essential for the maintenance of genomic stability, these proteins may synergistically function in tumor suppression by regulating these processes.

The physiological functions of caspase-2 have remained elusive since its discovery two decades ago (1–3). This is partly because of the lack of a clear phenotype in *caspase-2* KO (*Casp2*$^{-/-}$) mice that display only minor, tissue-specific apoptosis defects (4). We have previously demonstrated that loss of caspase-2 accelerates lymphomagenesis in Eμ-*Myc* transgenic mice, providing experimental evidence for a tumor suppressor function for caspase-2 (5). Consistent with a role in tumor suppression, loss of caspase-2 expression and function has been detected in various human cancers and has been associated with poor prognosis and drug resistance (6). From our previous work, we have also demonstrated that *caspase-2*–deficient mouse embryonic fibroblasts (MEFs) display aberrant proliferation, persistent DNA damage, and cell cycle checkpoint defects (7). Furthermore, *Casp2*$^{-/-}$ MEFs and lymphomas derived from Eμ-*Myc*/*Casp2*$^{-/-}$ mice exhibit increased aneuploidy, suggesting that caspase-2 is important for the maintenance of genomic stability (7). Our previous studies indicate that attenuated p53 induction and activity observed in *Casp2*$^{-/-}$ MEFs following DNA damage may contribute to these defects (7).

Strict regulation of cell cycle progression and preservation of genomic integrity are essential for maintaining cell homeostasis and preventing cell transformation (8). This is exemplified in cancer cells, which frequently display elevated levels of basal DNA damage, chromosomal instability, and aberrant proliferation (9). To protect against these detrimental effects, cells have evolved complex tumor suppressor networks to eliminate potentially malignant cells and prevent the transmission of mutations (8). Ataxia telangiectasia (A-T) mutated (ATM) kinase is a core component of these pathways and has an essential role in sensing DNA double-strand breaks and transducing downstream signals that activate the DNA repair and cell cycle checkpoint machinery (10). ATM has also been shown to be directly activated by oxidative stress through a mechanism distinct to that of activation by DNA breaks (11). Upon activation by reactive oxygen species (ROS), ATM stimulates the production of NADPH, thereby regulating cellular redox homeostasis during oxidative insult (12). Interestingly, *Casp2*$^{-/-}$ mice show premature aging-related traits, including oxidative tissue damage and a reduced ability to tolerate stress, implicating caspase-2 in the regulation of the antioxidant stress response (13, 14).

There is mounting evidence that the tumor suppressor function of caspase-2 is linked to its roles in the DNA damage response (DDR), oxidative defense system, and the maintenance of genomic stability (6). Given the overlapping functions of ATM and caspase-2 in these processes, we generated *Atm*/*caspase-2* double KO (*Atm*$^{-/-}$*Casp2*$^{-/-}$) mice to investigate whether caspase-2 and ATM genetically and functionally interact in tumor suppression and genome surveillance. *Atm*$^{-/-}$ mice recapitulate many clinical features of the rare human disease A-T, such as growth retardation, infertility, and hypersensitivity to ionizing radiation (15, 16). As in patients with A-T, *Atm*$^{-/-}$ mice are also prone to spontaneous lymphomagenesis (15, 16).

Here we show that *caspase-2* deficiency exacerbates somatic growth retardation in *Atm*$^{-/-}$ mice. Importantly, we found that loss of caspase-2 dramatically increases the incidence of

Significance

The cysteine protease caspase-2 has been implicated in the suppression of oncogene-mediated tumor formation. However, the mechanisms underlying the function of caspase-2 as a tumor suppressor are not well defined. In this study, we use a well-characterized mouse lymphoma model and demonstrate a critical role for caspase-2 in maintaining genome stability and in the suppression of tumorigenesis following loss of the essential DNA repair gene ataxia telangiectasia mutated (*Atm*). Our findings suggest that caspase-2 cooperates with ATM to suppress genomic instability, oxidative stress, and tumor progression.

Author contributions: J.P., L.D., and S.K. designed research; J.P., S.S., A.K.V., M.G., and C.H.W. performed research; D.K.H. and M.F.L. contributed new reagents/analytic tools; J.P., S.S., A.K.V., D.K.H., L.D., and S.K. analyzed data; and J.P., L.D., and S.K. wrote the paper.

The authors declare no conflict of interest.

*This Direct Submission article had a prearranged editor.

[1]L.D. and S.K. contributed equally to this work.

[2]To whom correspondence should be addressed. E-mail: sharad.kumar@health.sa.gov.au.

This article contains supporting information online at www.pnas.org/lookup/suppl/doi:10.1073/pnas.1311947110/-/DCSupplemental.

lymphomagenesis in $Atm^{-/-}$ mice. Furthermore, thymic lymphomas derived from $Atm^{-/-}Casp2^{-/-}$ mice displayed an increased proliferative capacity, extensive aneuploidy, and elevated levels of intracellular ROS. These results demonstrate that caspase-2 is a suppressor of lymphomas in $Atm^{-/-}$ mice and provide further direct evidence for a tumor suppressor function for caspase-2. Importantly, we also demonstrate that this function is linked to the maintenance of genomic stability, shedding new light on the physiological significance of caspase-2 in protecting against tumorigenesis.

Results

***Caspase-2* Deficiency Enhances Growth Retardation and Causes Perinatal Lethality in *Atm*$^{-/-}$ Mice.** To further investigate the role of caspase-2 in tumor suppression, we used $Atm^{-/-}$ mice to generate $Atm^{-/-}Casp2^{-/-}$ double-KO mice. This was achieved by intercrossing $Atm^{+/-}Casp2^{-/-}$ mice. Consistent with previous studies (15, 16), expected Mendelian ratios were observed from $Atm^{+/-} \times Atm^{+/-}$ intercrosses (Table 1). However, analysis of progeny from $Atm^{+/-}Casp2^{-/-}$ intercrosses revealed that only 23 (10%) $Atm^{-/-}Casp2^{-/-}$ mice were recovered at birth from a total of 230 offspring, a 60% reduction from the expected frequency (25%; Table 1). Interestingly, analysis of genotype frequencies from $Atm^{+/-}Casp2^{-/-}$ intercrosses at embryonic day 18.5 (E18.5) demonstrated that $Atm^{-/-}Casp2^{-/-}$ fetuses were present at the expected Mendelian ratios (Table 1). Furthermore, $Atm^{-/-}Casp2^{-/-}$ fetuses were alive at E18.5 as determined by their response to toe-pinch stimulus. These observations indicate that $Atm^{-/-}Casp2^{-/-}$ offspring die soon after birth. To assess the reason for this lethality, we carefully examined serial sections of E18.5 $Atm^{-/-}Casp2^{-/-}$, $Atm^{-/-}$, $Casp2^{-/-}$, and WT fetuses. We failed to see any specific phenotype in $Atm^{-/-}Casp2^{-/-}$ fetuses (Figs. S1 and S2).

To assess somatic animal growth, WT, $Atm^{-/-}$, $Casp2^{-/-}$, and $Atm^{-/-}Casp2^{-/-}$ mice were weighed weekly from 2 to 18 wk of age. Consistent with previous studies (15, 16) we observed a 20% to 25% reduction in the body weight of male and female $Atm^{-/-}$ mice compared with WT littermates (Fig. 1 *A*–*C*). Male and female $Atm^{-/-}Casp2^{-/-}$ mice displayed a further 10% to 15% reduction in body weight compared with sex-matched $Atm^{-/-}$ controls (Fig. 1 *A*–*C*). This additive growth defect was observed before weaning and persisted throughout adulthood. Also, $Casp2^{-/-}$ mice also displayed a minor growth defect compared with WT mice, although this trend reached statistical significance only in females. Taken together, these data demonstrate that combined loss of caspase-2 and ATM exacerbates growth retardation and causes perinatal lethality in *Atm*-deficient mice. Although the growth retardation phenotype in $Atm^{-/-}$ mice has been known for many years (15, 16), the mechanism of such a defect remains unknown. Similarly, examination of $Atm^{-/-}Casp2^{-/-}$ mice did not provide any phenotypic clues to enhanced growth retardation. We noticed that the majority of the $Atm^{-/-}Casp2^{-/-}$ animals at birth were frail and unable to compete for feeding and were routinely culled by their mothers. Thus, although the mechanism of retarded growth remains to be established, the perinatal lethality may simply be a result of weak constitution of some of the $Atm^{-/-}Casp2^{-/-}$ pups.

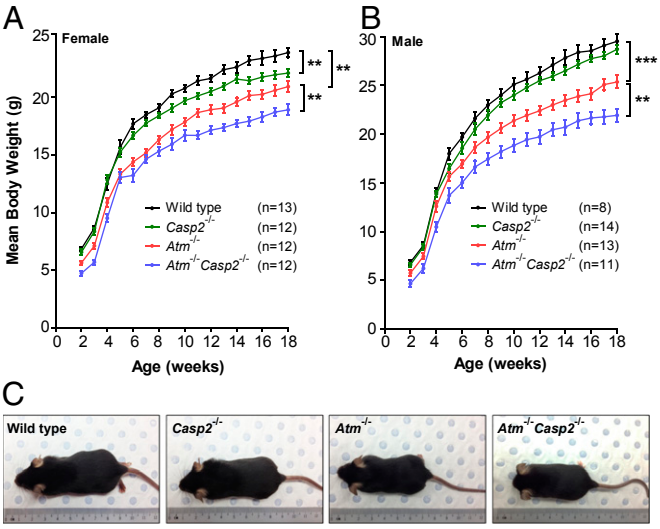

Fig. 1. *Caspase-2* deficiency enhances growth retardation in $Atm^{-/-}$ mice. Male and female mice were weighed weekly from 2 to 18 wk of age. Growth curves showing mean body weights for (*A*) females and (*B*) males of indicated genotypes. Data represented as mean ± SEM (**$P < 0.01$ and ***$P < 0.001$). (*C*) Representative images of 6-wk-old male mice showing size differences between genotypes.

Table 1. Genotype frequencies from mouse intercrosses

Genotype	Observed (%)	Expected (%)	*P* value
Cross: $Atm^{+/-} \times Atm^{+/-}$ (n = 284; birth)			
$Atm^{+/+}$	74 (26.1)	71 (25.0)	0.0853
$Atm^{+/-}$	155 (54.6)	142 (50.0)	
$Atm^{-/-}$	55 (19.3)	71 (25.0)	
Cross: $Atm^{+/-}Casp2^{-/-} \times Atm^{+/-}Casp2^{-/-}$ (n = 230; birth)			
$Atm^{+/+}Casp2^{-/-}$	70 (30.4)	57.5 (25.0)	0.000001
$Atm^{+/-}Casp2^{-/-}$	137 (59.6)	115 (50.0)	
$Atm^{-/-}Casp2^{-/-}$	23 (10.0)	57.5 (25.0)	
Cross: $Atm^{+/-}Casp2^{-/-} \times Atm^{+/-}Casp2^{-/-}$ (n = 62; E18.5)			
$Atm^{+/+}Casp2^{-/-}$	16 (25.8)	15.5 (25.0)	0.908
$Atm^{+/-}Casp2^{-/-}$	32 (51.6)	31 (50.0)	
$Atm^{-/-}Casp2^{-/-}$	14 (22.6)	15.5 (25.0)	

Observed and expected numbers of offspring generated from $Atm^{+/-} \times Atm^{+/-}$ crosses at birth and from $Atm^{+/-}Casp2^{-/-} \times Atm^{+/-}Casp2^{-/-}$ crosses at birth and E18.5. Expected and observed frequencies are indicated in parentheses. Statistical comparison was performed by χ^2 test.

Combined Loss of Caspase-2 and ATM Augments Lymphomagenesis. We have previously shown that *caspase-2* deficiency accelerates lymphomagenesis in Eμ-*Myc* transgenic mice (5). Previous reports show that *caspase-2* deficiency does not appear to affect tumor development induced by low dose γ-radiation or 3-methylcholanthrene (17). More recently, it was shown that deletion of *caspase-2* in murine mammary tumor virus transgenic mice accelerates tumorigenesis, showing that caspase-2 is also a suppressor of epithelial tumors (18). To further investigate the tumor suppressor function of caspase-2 specifically in the DDR and oxidative stress pathways, cohorts of $Atm^{-/-}$ and $Atm^{-/-}Casp2^{-/-}$ mice were generated and monitored for tumor development over a 1-y period. Under pathogen-free conditions, 12 of 38 $Atm^{-/-}$ mice (31.6%) developed spontaneous tumors with an average onset of 30.8 wk (Fig. 2 *A* and *B*). Notably, loss of caspase-2 dramatically enhanced the incidence of tumorigenesis in $Atm^{-/-}$ mice. Within 1 y, 14 of 22 $Atm^{-/-}Casp2^{-/-}$ mice (63.6%) developed tumors, with an average onset of 25.9 wk (Fig. 2 *A* and *B*). Both $Atm^{-/-}$ and $Atm^{-/-}Casp2^{-/-}$ mice predominately developed lymphomas of the thymus, with no differences observed in the histopathology of these lymphomas between genotypes (Fig. 2*C*). We also observed a small proportion of nonthymic lymphomas in both genotypes, which presented as hepatosplenomegaly and tumors of the lymph nodes. WT and $Casp2^{-/-}$ mice in a C57BL/6 background do not develop spontaneous tumors within 1 y under the same pathogen-free conditions (13).

Both $Atm^{-/-}$ and $Atm^{-/-}Casp2^{-/-}$ lymphomas were highly aggressive and infiltrated various secondary sites including the lungs, kidney, liver, and peripheral blood (Fig. S3*A*). Peripheral

MEDICAL SCIENCES

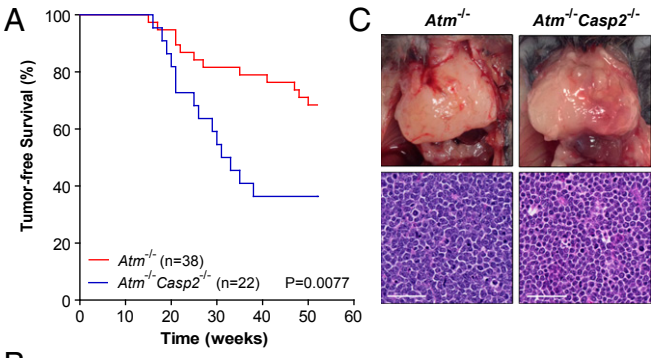

B

Genotype	Mice with Thymic Lymphomas	Mice with Non-thymic Lymphomas	Incidence at 1 year (%)	Average Onset (weeks)
Atm$^{-/-}$	8	4	31.6	30.8
Atm$^{-/-}$*Casp2*$^{-/-}$	12	2	63.6	25.9

Fig. 2. *Caspase-2* deficiency accelerates lymphomagenesis in *Atm*$^{-/-}$ mice. (*A*) Kaplan–Meier plot comparing percentage tumor-free survival in cohorts of *Atm*$^{-/-}$ (n = 38) and *Atm*$^{-/-}$*Casp2*$^{-/-}$ (n = 22) mice (P = 0.0077, log rank test). (*B*) Comparison of tumor types, incidence, and onset. (*C*) Representative images of *Atm*$^{-/-}$ and *Atm*$^{-/-}$*Casp2*$^{-/-}$ thymic lymphomas and H&E-stained thymic lymphoma sections (magnification of 40×) showing tumor cell morphology. (Scale bar: 50 μm.) No spontaneous tumor development was observed in WT or *Casp2*$^{-/-}$ mice over a 1-y period in the same pathogen-free animal facility.

blood lymphocyte counts were not significantly different between tumor-laden *Atm*$^{-/-}$ and *Atm*$^{-/-}$*Casp2*$^{-/-}$ mice, indicating comparable tumor burdens (Fig. S3*B*). Immunophenotyping and histological analysis revealed that thymic lymphomas derived from both *Atm*$^{-/-}$ and *Atm*$^{-/-}$*Casp2*$^{-/-}$ mice were predominantly composed of immature CD4^{+}CD8^{+} lymphoblastic T cells (also expressing the pan T-cell marker CD90.2; Fig. S4). Therefore, although *caspase-2* deficiency did not affect the metastatic potential, immunophenotype, or morphology of thymic lymphomas, loss of caspase-2 dramatically increased the incidence of tumorigenesis in *Atm*$^{-/-}$ mice.

Caspase-2 Deficiency Confers a Proliferative Advantage in *Atm*$^{-/-}$ Lymphomas. As caspase-2 has been suggested to contribute to regulation of cell cycle progression (7, 18) and *Casp2*$^{-/-}$ MEFs proliferate at a slightly faster rate than their WT counterparts (5, 7), we assessed the proliferative capacity of *Atm*$^{-/-}$*Casp2*$^{-/-}$ tumors. The proportion of actively proliferating cells, as determined by proliferating cell nuclear antigen (PCNA) expression, was significantly increased in *Atm*$^{-/-}$*Casp2*$^{-/-}$ thymic lymphomas (81.5%) compared with *Atm*$^{-/-}$ thymic lymphomas (69.3%; Fig. 3*A*). Interestingly, we observed comparable numbers of apoptotic cells in *Atm*$^{-/-}$ and *Atm*$^{-/-}$*Casp2*$^{-/-}$ thymic lymphomas as assessed by TUNEL immunohistochemistry (Fig. 3*B*). These data demonstrate that the loss of caspase-2 does not appear to affect apoptosis but enhances the proliferative capacity of *Atm*$^{-/-}$ tumors, suggesting that proliferative defects may contribute to the accelerated tumorigenesis observed in *Atm*$^{-/-}$*Casp2*$^{-/-}$ mice.

Given that ATM and caspase-2 are both important regulators of antioxidant defense and the DDR pathway, we next assessed how *Atm*$^{-/-}$ and *Atm*$^{-/-}$*Casp2*$^{-/-}$ thymic lymphoma cells responded to genotoxic and oxidative stress. Primary cells isolated from *Atm*$^{-/-}$ and *Atm*$^{-/-}$*Casp2*$^{-/-}$ thymic lymphomas were cultured and treated with 5 Gy γ-radiation and the phosphorylation of a number of ATM substrates was assessed by immunoblotting (Fig. S5*A*). As expected, in response to dsDNA breaks, activation of downstream effectors involved in DNA repair and cell cycle arrest (Chk1, SMC1, and KAP-1) was significantly ablated in *Atm*$^{-/-}$ lymphoma cells (Fig. S5*A*). However, we did not observe any further impairment in the activation of these proteins in *Atm*$^{-/-}$*Casp2*$^{-/-}$ lymphoma cells.

As the loss of caspase-2 is associated with impaired p53 signaling in MEFs (7), we assessed p53 and p21 protein levels in primary *Atm*$^{-/-}$ and *Atm*$^{-/-}$*Casp2*$^{-/-}$ thymic lymphomas. However, we did not observe any differences between the genotypes suggesting that loss of caspase-2 does not affect p53 activity in *Atm*-deficient tumors (Fig. S5*B*). We also examined the extent of cell death and found that apoptosis was rapidly induced at comparable levels in *Atm*$^{-/-}$ and *Atm*$^{-/-}$*Casp2*$^{-/-}$ thymic lymphoma cells following treatment with γ-radiation and the ROS inducer menadione (Fig. 3 *C* and *D*). Taken together, these data demonstrate that loss of caspase-2 does not affect DNA damage or ROS-induced apoptosis in *Atm*$^{-/-}$ tumors in vitro.

***Atm*$^{-/-}$*Casp2*$^{-/-}$ Lymphomas and Premalignant T Lymphocytes Display Enhanced Aneuploidy.** To assess whether caspase-2 influences genomic stability in *Atm*$^{-/-}$ tumors, we performed cytogenetic analysis on freshly isolated thymic lymphomas. Metaphases from tumor cells were categorized as diploid (n = 40), low-grade

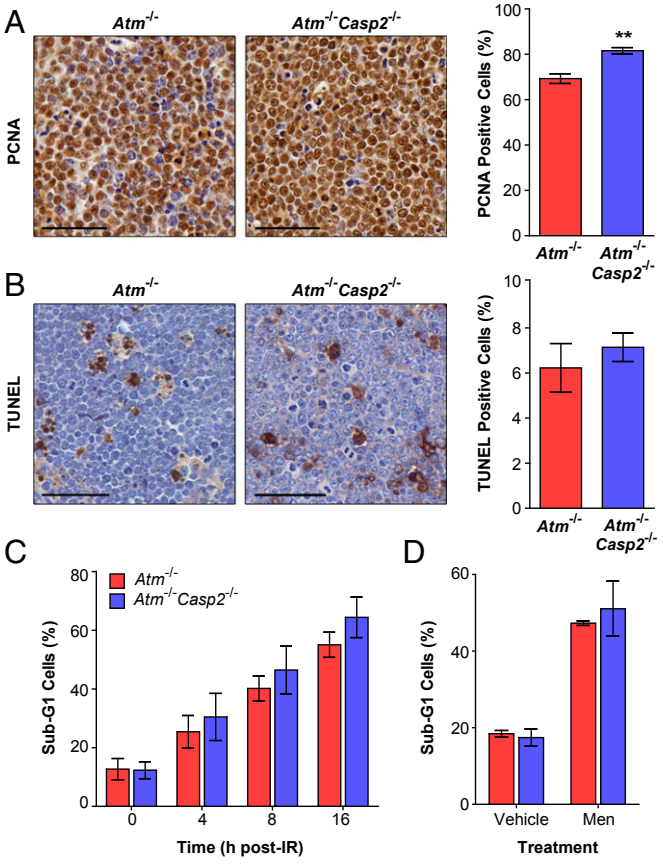

Fig. 3. Loss of caspase-2 enhances proliferation without affecting cell death in *Atm*$^{-/-}$ lymphomas. Representative images (magnification of 40×) and quantification of (*A*) PCNA immunohistochemistry performed on thymic lymphoma sections derived from *Atm*$^{-/-}$ (n = 5) and *Atm*$^{-/-}$*Casp2*$^{-/-}$ (n = 5) mice and (*B*) TUNEL immunohistochemistry performed on thymic lymphoma sections derived from *Atm*$^{-/-}$ (n = 7) and *Atm*$^{-/-}$*Casp2*$^{-/-}$ (n = 10) mice. (Scale bars: 50 μm.) A total of 900 to 1,500 cells were blind-counted over four separate fields of view for each tumor. (*C*) Flow cytometry analysis of apoptosis in (C) *Atm*$^{-/-}$ (n = 3) and *Atm*$^{-/-}$*Casp2*$^{-/-}$ (n = 3) primary lymphoma cell lines following γ-irradiation (5 Gy) and (*D*) *Atm*$^{-/-}$ (n = 2) and *Atm*$^{-/-}$*Casp2*$^{-/-}$ (n = 3) primary lymphoma cell lines following 8 h treatment with vehicle (DMSO) or menadione (10 μM). Cells with a sub-G1 DNA content were gated as apoptotic. Data presented as mean ± SEM (**P < 0.01, Student t test).

aneuploid (loss or gain of as many as 9 chromosomes), or high-grade aneuploid (loss or gain of 10 or more chromosomes). It has previously been shown that thymic lymphomas derived from $Atm^{-/-}$ mice are diploid, with a mean chromosome number of 40 (19). Consistent with this, the majority of metaphases (82.9%) from all $Atm^{-/-}$ thymic lymphomas analyzed showed diploid karyotypes, with only 14.6% and 2.5% of metaphases displaying low- and high-grade aneuploidy, respectively (Fig. 4 *A* and *B* and Fig. S6*A*). In contrast, $Atm^{-/-}Casp2^{-/-}$ thymic lymphomas displayed a significant increase in the proportion of metaphases with low-grade (58.9%) and high-grade (13.9%) aneuploidy, which coincided with a marked reduction in the proportion of diploid metaphases (27.2%; Fig. 4 *A* and *B* and Fig. S6*A*). These observations provide direct evidence that loss of caspase-2 promotes chromosomal instability in vivo.

To further investigate whether loss of genomic stability contributes to the enhanced lymphomagenesis in $Atm^{-/-}Casp2^{-/-}$ mice, we performed cytogenetic analysis on mitogen-activated splenic and thymic T lymphocytes derived from 13 to 14 wk old premalignant mice. Karyotype distributions of $Atm^{-/-}$ splenocytes and thymocytes were indistinguishable from the WT and $Casp2^{-/-}$ controls (Fig. 4 *C* and *D* and Fig. S6 *B* and *C*). Strikingly, we observed a reduced frequency of diploid metaphases and concomitant increase in the proportion of aneuploid metaphases in $Atm^{-/-}Casp2^{-/-}$ splenocytes and thymocytes compared with $Atm^{-/-}$ controls (Fig. 4 *C* and *D* and Fig. S6 *B* and *C*). These observations demonstrate that loss of caspase-2 promotes genomic instability even before tumor onset in $Atm^{-/-}$ mice. Given that we have previously shown that $Casp2^{-/-}$ MEFs and lymphomas derived from Eμ-*Myc*/$Casp2^{-/-}$ mice display reduced telomere length (7), we performed FISH to assess telomere length in thymic lymphomas. However, we did not observe any significant differences in telomere length or loss between $Atm^{-/-}$ and $Atm^{-/-}Casp2^{-/-}$ thymic lymphomas (Fig. S7), suggesting that telomere dysfunction does not contribute to the chromosome instability in this model.

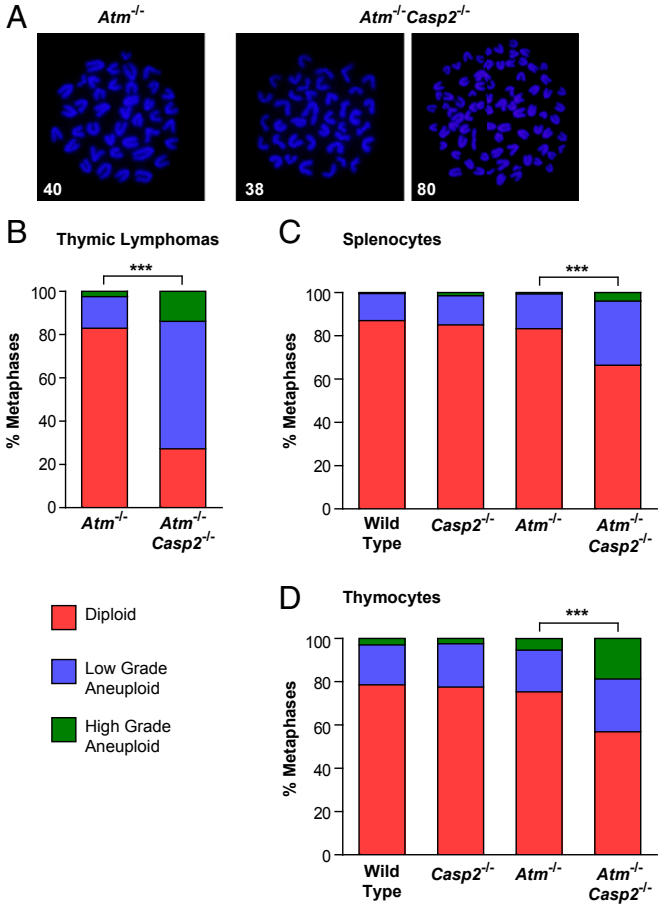

Fig. 4. Enhanced genomic instability in $Atm^{-/-}Casp2^{-/-}$ lymphomas and premalignant lymphocytes. (*A*) Representative fluorescent images (magnification of 100×) of DAPI-stained metaphase spreads (with chromosome counts indicated) from $Atm^{-/-}$ and $Atm^{-/-}Casp2^{-/-}$ thymic lymphomas. Quantification of metaphases showing frequencies of diploid, low-grade aneuploid, and high-grade aneuploid karyotypes in (*B*) thymic lymphomas derived from $Atm^{-/-}$ ($n = 3$) and $Atm^{-/-}Casp2^{-/-}$ ($n = 8$) mice and (*C*) splenocytes and (*D*) thymocytes derived from WT ($n = 4$), $Casp2^{-/-}$ ($n = 4$), $Atm^{-/-}$ ($n = 3$), and $Atm^{-/-}Casp2^{-/-}$ ($n = 5$) premalignant mice. A total of 80 (thymic lymphomas) and 50 (splenocytes and thymocytes) metaphases were counted per mouse (***$P < 0.001$, χ^2 test).

Increased Oxidative Damage in $Atm^{-/-}Casp2^{-/-}$ Lymphomas. Aneuploidy is known to alter cellular energy metabolism and cause increased ROS production (20). Given that ATM and caspase-2 are known to regulate the oxidative stress response and that $Atm^{-/-}Casp2^{-/-}$ tumors exhibit extensive aneuploidy, we assessed oxidative damage in thymic lymphomas derived from $Atm^{-/-}$ and $Atm^{-/-}Casp2^{-/-}$ mice. Protein carbonyls and 8-hydroxy-2-deoxy guanosine (8-OHdG) are the products of oxidatively modified protein and DNA, respectively, and are robust markers for oxidative damage. We observed significantly increased levels of protein carbonyls and 8-OHdG in $Atm^{-/-}Casp2^{-/-}$ thymic lymphomas compared with $Atm^{-/-}$ thymic lymphomas (Fig. 5 *A* and *B*). *Atm*-deficient splenocytes and thymocytes displayed increased protein carbonyl levels compared with WT controls (Fig. S8). However, we did not observe any differences in protein carbonyl levels between $Atm^{-/-}$ and $Atm^{-/-}Casp2^{-/-}$ splenocytes and thymocytes from premalignant mice (Fig. S8). These observations imply that the increased oxidative damage observed in $Atm^{-/-}Casp2^{-/-}$ thymic lymphomas is acquired at the malignant stage, rather than in premalignant cells.

In response to oxidative stress, cells up-regulate a highly conserved network of antioxidant genes to neutralize ROS and prevent oxidative damage (21). The mitochondrial-localized antioxidant enzymes manganese superoxide dismutase (Sod2), peroxiredoxin III (Prdx3), and catalase (Cat) form an essential axis of these pathways (21). In addition, cells also up-regulate the stress-responsive genes of the sestrin family to mediate antioxidant defense (22). Not surprisingly, the increased oxidative stress observed in $Atm^{-/-}Casp2^{-/-}$ tumors coincided with a significant increase in the transcript levels of these antioxidant genes (Fig. 5*C*). Although a trend was observed, the difference in *Cat* levels did not reach statistical significance (Fig. 5*C*). Moreover, we also observed increased transcript levels of Sestrin 1 and Sestrin 2, further indicating the presence of elevated oxidative stress in $Atm^{-/-}Casp2^{-/-}$ tumors (Fig. 5*C*). These results demonstrate that ATM and caspase-2 cooperate to suppress oxidative stress in vivo.

Discussion

In this study, we used $Atm^{-/-}$ mice as a non–oncogene-driven model of spontaneous thymic lymphomagenesis and show that deletion of *caspase-2* enhances the incidence of lymphomagenesis in $Atm^{-/-}$ mice. We also observed an increased proliferative capacity, extensive chromosomal instability, and increased oxidative damage in $Atm^{-/-}Casp2^{-/-}$ tumors. Furthermore, our work uncovered that loss of caspase-2 enhances growth retardation in $Atm^{-/-}$ mice.

Several DNA repair gene KO mouse strains have been created in an *Atm*-null background to study their function in vivo. Similar to the $Atm^{-/-}Casp2^{-/-}$ mice, many of these double-KO strains are synthetic lethal, including $p53^{-/-}Atm^{-/-}$, $PARP1^{-/-}Atm^{-/-}$, $Lig4^{-/-}Atm^{-/-}$, and $DNA\text{-}PKcs^{-/-}Atm^{-/-}$ mice (23–26). Although histological inspection of fetal tissues did not reveal any obvious anomalies that could explain the death of $Atm^{-/-}Casp2^{-/-}$ mice, it

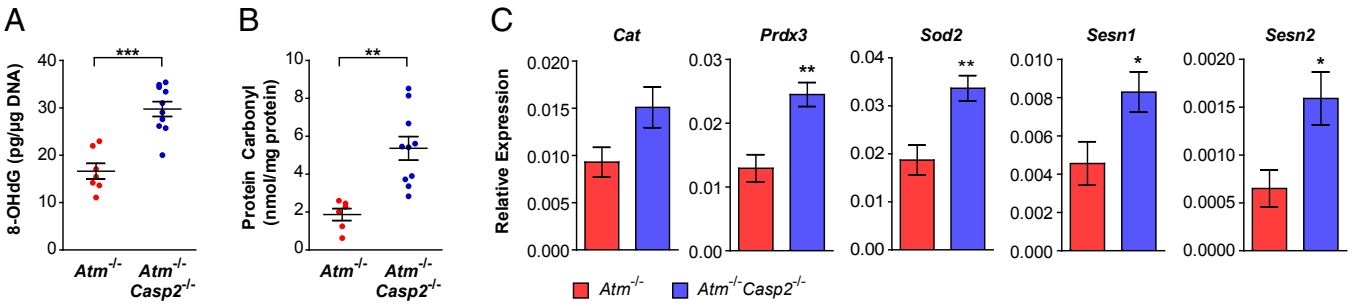

Fig. 5. Increased oxidative damage in $Atm^{-/-}Casp2^{-/-}$ lymphomas. (*A*) 8-OHdG and (*B*) protein carbonyl levels in $Atm^{-/-}$ ($n = 6$–7) and $Atm^{-/-}Casp2^{-/-}$ ($n = 10$) thymic tumors. Each point represents an individual tumor. (*C*) Quantitative PCR analysis of superoxide dismutase 2 (*Sod2*), peroxiredoxin 3 (*Prdx3*), *Sesn1* (Sestrin 1), *Sesn2* (Sestrin 2), and *Cat* (Catalase) expression in $Atm^{-/-}$ ($n = 6$) and $Atm^{-/-}Casp2^{-/-}$ ($n = 10$) thymic lymphomas. Expression is relative to β-actin levels. Data represented as mean ± SEM (*$P < 0.05$, **$P < 0.01$, and ***$P < 0.001$, Student *t* test).

is likely that enhanced growth retardation in the $Atm^{-/-}Casp2^{-/-}$ animals contributes to the lethality in newborn pups.

Several studies have reported increased levels of ROS and chronic oxidative stress in tissues from $Atm^{-/-}$ mice (27, 28). Aged $Casp2^{-/-}$ mice have also been shown to have an impaired antioxidant defense system and elevated levels of ROS, which is believed to cause premature aging (13, 14). Therefore, it is possible that combined loss of ATM and caspase-2 exacerbates oxidative damage, leading to enhanced retardation of somatic growth and perinatal lethality in $Atm^{-/-}Casp2^{-/-}$ mice. In support of the hypothesis that a poor response to oxidative stress might cause growth retardation, mutation of genes involved in the oxidative stress response have previously been shown to cause developmental retardation in humans (29).

Given the overlapping functions of ATM and caspase-2 in the DDR, antioxidant defense, and tumor suppression, we hypothesized that deletion of both these genes would accelerate tumorigenesis. Indeed, we show that deletion of *caspase-2* dramatically enhanced the incidence of lymphomagenesis in $Atm^{-/-}$ mice. These important findings demonstrate that caspase-2 is a suppressor of not just *Myc*-driven, but also non–*Myc*-driven, lymphomagenesis.

Consistent with previous studies (5, 7, 18), we observed an increased proliferation index in $Atm^{-/-}Casp2^{-/-}$ tumors, suggesting that caspase-2 deletion, when combined with other oncogenic lesions, confers a proliferative advantage in vivo. Taken together, these data indicate that caspase-2 may function in cell cycle regulation, which may partly contribute to its tumor suppressor function. Importantly, *caspase-2* deficiency does not affect DNA double strand break signaling or apoptosis induced by genotoxic and oxidative stress in $Atm^{-/-}$ tumor cells in vitro. Furthermore, we provide evidence that defective cell death pathways or impaired p53 signaling are unlikely to contribute to the increased tumor incidence in $Atm^{-/-}Casp2^{-/-}$ mice. However, we cannot rule out the possibility that *caspase-2* deficiency renders premalignant $Atm^{-/-}Casp2^{-/-}$cells harboring aneuploid karyotypes, resistant to cell death.

In this study, we demonstrate that *caspase-2* deficiency is associated with chromosomal instability in vivo. Importantly, we observed increased genomic instability even in premalignant lymphocytes providing further evidence that loss of genomic stability is not merely a consequence, but rather a cause of the enhanced tumorigenesis in $Atm^{-/-}Casp2^{-/-}$ mice. This important finding suggests that caspase-2 may exert its tumor suppressor function through the maintenance of genomic stability. There is strong evidence that aneuploid cells experience proteotoxic stress as a result of imbalances in gene dosage, which leads to the generation of ROS (20). In line with this, we observed increased oxidative damage to DNA and proteins as assessed by 8-OHdG and protein carbonyl levels, respectively. Interestingly, we did not observe increased oxidative damage in premalignant lymphocytes derived from $Atm^{-/-}Casp2^{-/-}$ mice compared with $Atm^{-/-}$ controls. Hence, excessive oxidative damage appears to follow aneuploidization and is a phenotype acquired in malignant cells.

Increased levels of ROS is a hallmark of the cancer phenotype, and there is mounting evidence to suggest that cancer cells experiencing oxidative stress undergo extensive reprogramming of mechanisms regulating redox homeostasis (20). It has been suggested that this reprogramming may represent an adaptive response that maintains ROS levels below a toxic threshold, while still inflicting oxidative damage, thereby permitting survival of tumor cells experiencing chronic oxidative stress (20). The observed increase in oxidative damage in $Atm^{-/-}Casp2^{-/-}$ tumors coincided with up-regulation of various stress-responsive genes involved in ROS detoxification. Interestingly, a recent study has shown that elevated levels of ROS in aneuploid cells triggers an ATM-dependent response that protects against aneuploidy-induced tumorigenesis (30). Furthermore, the levels of ROS were shown to be highly correlated with the extent of aneuploidy (30). Our data further predict that aneuploidy and oxidative damage induced by *caspase-2* deficiency in the absence of ATM would allow these damaged cells to acquire additional oncogenic lesions more readily. Furthermore, these observations are consistent with a model by which ATM and caspase-2 operate in parallel tumor suppressor pathways that protect against oxidative stress and aneuploidy (Fig. S9). Therefore, disruption of these pathways may explain the enhanced incidence of lymphomagenesis in $Atm^{-/-}Casp2^{-/-}$ mice.

One of the major open questions in the field is whether the functions of caspase-2 in the DDR, maintenance of genomic stability, and tumor suppression are solely based on its role in apoptosis, or whether caspase-2 regulates these processes through nonapoptotic mechanisms. Nonetheless, our work here shows that loss of caspase-2 in a sensitized background promotes the acquisition of chromosomal instability and oxidative damage that promotes tumorigenesis. Consistent with these observations, our previous studies demonstrate that, although *caspase-2* deficiency renders primary MEFs more susceptible to oncogene-induced transformation and increases the tumorigenic potential of transformed cells, loss of caspase-2 is not sufficient to initiate spontaneous tumorigenesis in vivo (5, 13). Taken together, these findings provide further evidence that one of the primary functions of this enigmatic caspase is protection against cellular stress conditions that promote tumorigenesis.

Materials and Methods

Mice. All animals were maintained in specific pathogen-free conditions in a 12 h/12 h light/dark cycle and treated in accordance with protocols approved by the SA Pathology/Central Northern Adelaide Health Services Animal Ethics Committee. After weaning at postnatal day 18 to 21, mice were separated

according to sex, and food and water were provided ad libitum. *Casp2*$^{-/-}$ (31) and *Atm*$^{+/-}$ (15) mice have been backcrossed to a C57BL/6 background for at least 20 generations. Because *Atm*$^{-/-}$ mice are infertile, *Atm*$^{+/-}$ mice were intercrossed to generate *Atm*$^{-/-}$ offspring. *Atm*$^{+/-}$ mice were then crossed with *Casp2*$^{-/-}$ mice to generate compound heterozygotes (*Atm*$^{+/-}$*Casp2*$^{+/-}$), which were subsequently crossed with *Casp2*$^{-/-}$ mice to obtain *Atm*$^{+/-}$*Casp2*$^{-/-}$ offspring. *Atm*$^{+/-}$*Casp2*$^{-/-}$ mice were then intercrossed to generate the following genotypes: *Atm*$^{+/+}$*Casp2*$^{-/-}$; *Atm*$^{+/-}$*Casp2*$^{-/-}$; and *Atm*$^{-/-}$*Casp2*$^{-/-}$. Mice displaying signs of tumor burden such as hunched posture, weight loss, ruffled coats, and respiratory distress were humanely killed, and tumor presence was confirmed by autopsy. Tissues were harvested and snap-frozen in liquid nitrogen or fixed in 10% (vol/vol) neutral buffered formalin. Primary splenocyte and thymocyte cell suspensions were isolated from 13- to 14-wk-old premalignant mice. More details are provided in *SI Materials and Methods*.

Flow Cytometry. Samples were prepared and analyzed as described in *SI Materials and Methods*.

8-OHdG/Protein Carbonyl Measurements. Protein and DNA oxidation was quantified by using the Protein Carbonyl Colorimetric Assay Kit (cat. no. 10005020; Cayman Chemical) and 8-OHdG E1A Kit (cat. no. 589320; Cayman Chemical) according to the manufacturer's instructions. Details of sample preparation are provided in *SI Materials and Methods*.

Cytogenetic Analysis. Metaphase spreads were prepared from freshly isolated thymic lymphoma, splenocyte, and thymocyte cell suspensions as previously described (7). Images were captured using an epifluorescence microscope (model BX51; Olympus) and camera (U0CMAD3/CVM300; Olympus).

Quantitative PCR. Details of RNA extraction, cDNA synthesis, and primer sequences are provided in *SI Materials and Methods*.

Immunohistochemistry. Formalin-fixed, paraffin-embedded thymic lymphoma sections were deparaffinized in xylene and rehydrated in graded ethanol series. Endogenous peroxidase activity and nonspecific protein sites were blocked with 3% (vol/vol) H_2O_2/PBS solution and 5% (vol/vol) FBS/PBS solution with Tween-20, respectively. Tissue sections were incubated with anti-PCNA primary antibody (clone PC10; Cell Signaling Technology) diluted 1:250 in blocking solution overnight at 4 °C. Tissue sections were sequentially incubated with anti-mouse biotinylated secondary antibody (1:250 in blocking solution; GE Healthcare) and Avidin/Biotin Complex reagent (VectaStain) at room temperature. Peroxidase substrate (3,3′-diaminobenzidine) was added for color development, followed by counterstaining with Mayer hematoxylin solution (Sigma-Aldrich). Tissue sections were then dehydrated in graded ethanol series and coverslips mounted by using DePex mounting media. Detection of apoptotic cells by TUNEL was performed on formalin-fixed, paraffin-embedded thymic lymphoma sections as previously described (32). Digital images were acquired by using a NanoZoomer (Hamamatsu).

Statistical Analysis of Data. Nonlinear regression curve fitting was used for statistical analysis of mouse growth curves. Analysis of expected and observed frequencies of mouse genotype and karyotypes frequencies was performed by χ^2 test. Log-rank test and Kaplan–Meier analysis were used for comparison of mouse survival. Two-tailed unpaired Student *t* tests were used for used for all other analyses. Data are presented as mean ± SEM unless otherwise stated. $P < 0.05$ was considered statistically significant. All statistical analyses were performed by using GraphPad Prism Version 5.

ACKNOWLEDGMENTS. We thank staff at the SA Pathology animal facility for help with maintaining the mouse strains and Jim Manavis (SA Pathology) for TUNEL immunohistochemistry. This work was supported by National Health and Medical Research Council (NHMRC) Project Grants 1021456 and 1043057; an Australian Postgraduate Award (to J.P.); a Cancer Council Senior Research Fellowship (to L.D.), NHMRC Senior Research Fellowship 575512 (to A.K.V.), and NHMRC Senior Principal Research Fellowship 1002863 (to S.K.).

1. Kumar S, Tomooka Y, Noda M (1992) Identification of a set of genes with developmentally down-regulated expression in the mouse brain. *Biochem Biophys Res Commun* 185(3):1155–1161.
2. Kumar S, Kinoshita M, Noda M, Copeland NG, Jenkins NA (1994) Induction of apoptosis by the mouse Nedd2 gene, which encodes a protein similar to the product of the Caenorhabditis elegans cell death gene ced-3 and the mammalian IL-1 beta-converting enzyme. *Genes Dev* 8(14):1613–1626.
3. Wang L, Miura M, Bergeron L, Zhu H, Yuan J (1994) Ich-1, an Ice/ced-3-related gene, encodes both positive and negative regulators of programmed cell death. *Cell* 78(5):739–750.
4. Bergeron L, et al. (1998) Defects in regulation of apoptosis in caspase-2-deficient mice. *Genes Dev* 12(9):1304–1314.
5. Ho LH, et al. (2009) A tumor suppressor function for caspase-2. *Proc Natl Acad Sci USA* 106(13):5336–5341.
6. Puccini J, Dorstyn L, Kumar S (2013) Caspase-2 as a tumour suppressor. *Cell Death Differ* 20(9):1133–1139.
7. Dorstyn L, et al. (2012) Caspase-2 deficiency promotes aberrant DNA-damage response and genetic instability. *Cell Death Differ* 19(8):1288–1298.
8. Harper JW, Elledge SJ (2007) The DNA damage response: Ten years after. *Mol Cell* 28(5):739–745.
9. Hanahan D, Weinberg RA (2011) Hallmarks of cancer: The next generation. *Cell* 144(5):646–674.
10. Shiloh Y, Ziv Y (2013) The ATM protein kinase: Regulating the cellular response to genotoxic stress, and more. *Nat Rev Mol Cell Biol* 14(4):197–210.
11. Guo Z, Kozlov S, Lavin MF, Person MD, Paull TT (2010) ATM activation by oxidative stress. *Science* 330(6003):517–521.
12. Cosentino C, Grieco D, Costanzo V (2011) ATM activates the pentose phosphate pathway promoting anti-oxidant defence and DNA repair. *EMBO J* 30(3):546–555.
13. Shalini S, et al. (2012) Impaired antioxidant defence and accumulation of oxidative stress in caspase-2-deficient mice. *Cell Death Differ* 19(8):1370–1380.
14. Zhang Y, et al. (2007) Caspase-2 deficiency enhances aging-related traits in mice. *Mech Ageing Dev* 128(2):213–221.
15. Elson A, et al. (1996) Pleiotropic defects in ataxia-telangiectasia protein-deficient mice. *Proc Natl Acad Sci USA* 93(23):13084–13089.
16. Barlow C, et al. (1996) Atm-deficient mice: A paradigm of ataxia telangiectasia. *Cell* 86(1):159–171.
17. Manzl C, et al. (2012) PIDDosome-independent tumor suppression by Caspase-2. *Cell Death Differ* 19(10):1722–1732.
18. Parsons MJ, et al. (2013) Genetic deletion of caspase-2 accelerates MMTV/c-neu-driven mammary carcinogenesis in mice. *Cell Death Differ* 20(9):1174–1182.
19. Liyanage M, et al. (2000) Abnormal rearrangement within the alpha/delta T-cell receptor locus in lymphomas from Atm-deficient mice. *Blood* 96(5):1940–1946.
20. Gordon DJ, Resio B, Pellman D (2012) Causes and consequences of aneuploidy in cancer. *Nat Rev Genet* 13(3):189–203.
21. Kohen R, Nyska A (2002) Oxidation of biological systems: Oxidative stress phenomena, antioxidants, redox reactions, and methods for their quantification. *Toxicol Pathol* 30(6):620–650.
22. Budanov AV (2011) Stress-responsive sestrins link p53 with redox regulation and mammalian target of rapamycin signaling. *Antioxid Redox Signal* 15(6):1679–1690.
23. Gurley KE, Kemp CJ (2001) Synthetic lethality between mutation in Atm and DNA-PK (cs) during murine embryogenesis. *Curr Biol* 11(3):191–194.
24. Ménisser-de Murcia J, Mark M, Wendling O, Wynshaw-Boris A, de Murcia G (2001) Early embryonic lethality in PARP-1 Atm double-mutant mice suggests a functional synergy in cell proliferation during development. *Mol Cell Biol* 21(5):1828–1832.
25. Lee Y, Barnes DE, Lindahl T, McKinnon PJ (2000) Defective neurogenesis resulting from DNA ligase IV deficiency requires Atm. *Genes Dev* 14(20):2576–2580.
26. Xu Y, Yang EM, Brugarolas J, Jacks T, Baltimore D (1998) Involvement of p53 and p21 in cellular defects and tumorigenesis in Atm-/- mice. *Mol Cell Biol* 18(7):4385–4390.
27. Kamsler A, et al. (2001) Increased oxidative stress in ataxia telangiectasia evidenced by alterations in redox state of brains from Atm-deficient mice. *Cancer Res* 61(5):1849–1854.
28. Barlow C, et al. (1999) Loss of the ataxia-telangiectasia gene product causes oxidative damage in target organs. *Proc Natl Acad Sci USA* 96(17):9915–9919.
29. Basel-Vanagaite L, et al. (2012) Deficiency for the ubiquitin ligase UBE3B in a blepharophimosis-ptosis-intellectual-disability syndrome. *Am J Hum Genet* 91(6):998–1010.
30. Li M, et al. (2010) The ATM-p53 pathway suppresses aneuploidy-induced tumorigenesis. *Proc Natl Acad Sci USA* 107(32):14188–14193.
31. O'Reilly LA, et al. (2002) Caspase-2 is not required for thymocyte or neuronal apoptosis even though cleavage of caspase-2 is dependent on both Apaf-1 and caspase-9. *Cell Death Differ* 9(8):832–841.
32. Chua JS, Cowley CJ, Manavis J, Rofe AM, Coyle P (2012) Prenatal exposure to lipopolysaccharide results in neurodevelopmental damage that is ameliorated by zinc in mice. *Brain Behav Immun* 26(2):326–336.